Article

Electrochemical Synthesis, Crystal Structure, and Photomagnetic Properties of a Three-Dimensional Cyano-Bridged Copper–Molybdenum Complex

Toshiya Hozumi, Kazuhito Hashimoto, and Shin-ichi Ohkoshi

J. Am. Chem. Soc., **2005**, 127 (11), 3864-3869• DOI: 10.1021/ja044107o • Publication Date (Web): 25 February 2005

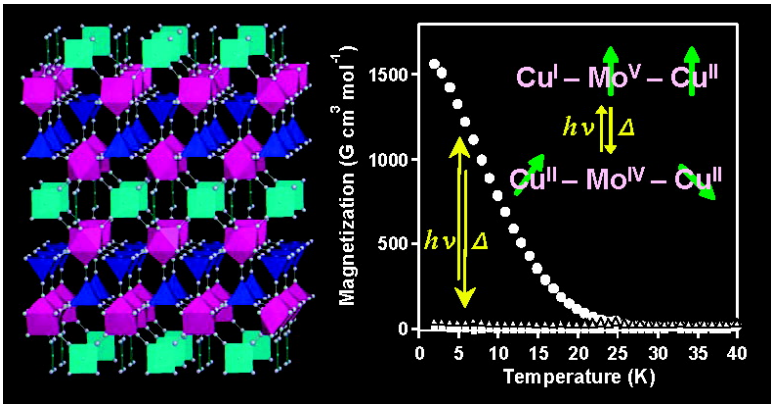

More About This Article

Additional resources and features associated with this article are available within the HTML version:

- Supporting Information
- Links to the 11 articles that cite this article, as of the time of this article download
- Access to high resolution figures
- Links to articles and content related to this article
- Copyright permission to reproduce figures and/or text from this article

View the Full Text HTML

J|A|C|S
ARTICLES
Published on Web 02/25/2005

Electrochemical Synthesis, Crystal Structure, and Photomagnetic Properties of a Three-Dimensional Cyano-Bridged Copper−Molybdenum Complex

Toshiya Hozumi,[†] Kazuhito Hashimoto,*[,†] and Shin-ichi Ohkoshi*[,†,‡]

Contribution from the Department of Applied Chemistry, School of Engineering, The University of Tokyo, 7-3-1 Hongo, Bunkyo-ku, Tokyo, Japan, and PRESTO, JST, 4-1-8 Honcho Kawaguchi, Saitama, Japan

Received September 28, 2004; E-mail: ohkoshi@light.t.u-tokyo.ac.jp; hashimoto@light.t.u-tokyo.ac.jp

Abstract: A single crystal of $Cs^{I}_{2}Cu^{II}_{7}[Mo^{IV}(CN)_8]_4 \cdot 6H_2O$ was electrochemically prepared on a Pt wire electrode with a constant potential of +500 mV vs Ag/AgCl electrode. X-ray single-crystal structural analysis showed that this compound consists of a three-dimensional cyano-bridged Cu−Mo bimetallic assembly with a tetragonal structure of *I*4/*mmm*. The coordination geometry of Mo^{IV} is bicapped trigonal prism, and that of Cu^{II} is five-coordinate of square pyramidal or four-coordinate of square planar. This compound was also prepared as a 0.2−3.0 μm thick film on a SnO_2-coated glass in the same electrochemical manner. When the sample, which shows paramagnetism due to Cu^{II} ($S = {}^1/_2$), was irradiated with 450−500 nm light at 5 K, spontaneous magnetization with a Curie temperature of 23 K was observed. This photoinduced change was recovered by a thermal treatment. In the infrared (IR) and electron spin resonance (ESR) spectra after light irradiation, variations in the stretching IR peak of CN bridged to Mo^{IV} and the paramagnetic ESR peak of Cu^{II} were observed, respectively. The data indicate that this photomagnetism is caused by the electron transfer from Mo^{IV} to Cu^{II} and the ferromagnetic ordering between Cu^{II} ($S = {}^1/_2$) and Mo^{V} ($S = {}^1/_2$).

1. Introduction

Optical control of magnetic properties is an issue of current interest in materials science.[1−9] A successful approach is to control the electronic state of a magnetic material. For example, magnetization is controlled when the oxidation numbers of transition metal ions within a magnetic material are varied by photoirradiation. In addition, the bistability of the electronic states is indispensable for observing photoinduced magnetization since the photoproduced state must persist even after photoirradiation is terminated. Along these lines, the photomagnetic properties of cyano-bridged metal assemblies have been studied,[2−9] that is, the photoinduced magnetization in cobalt−hexacyanoferrate,[3] cobalt−octacyanotungstate,[4] and copper−octacyanomolybdate,[5,6] photodemagnetization in iron−hexacyanochromate[7] and rubidium−manganese−hexacyanoferrate,[8] and a photoinduced magnetic pole inversion in iron−manganese−hexacyanochromate.[9] Furthermore, cyano-bridged metal assemblies[10] have been studied as functionalized molecule-based magnets. For example, hexacyanometalate-based magnets exhibit high magnetic phase transition temperatures[11] and unique magnetic behaviors.[12−15] Octacyanometalates $[M(CN)_8]^{n-}$ (M = Mo, W, ...) are also useful building blocks for functionalized molecule-based magnets since they can adopt three

[†] The University of Tokyo.
[‡] PRESTO.

(1) Decurtins, S.; Gütlich, P.; Köhler, C. P.; Spiering, H.; Hauser, A. *Chem. Phys. Lett.* **1984**, *105*, 1. (b) Decurtins, S.; Gütlich, P.; Hasselbach, K. M.; Spiering, H. *Inorg. Chem.* **1985**, *24*, 2174. (c) Gütlich, P.; Hauser, A.; Spiering, H. *Angew. Chem., Int. Ed. Engl.* **1994**, *33*, 2024.
(2) Ohkoshi, S.; Hashimoto, K. *J. Photochem. Photobiol., C* **2001**, *2*, 71.
(3) Sato, O.; Iyoda, T.; Fujishima, A.; Hashimoto, K. *Science* **1996**, *272*, 704. (b) Bleuzen, A.; Lomenech, C.; Escax, V.; Villain, F.; Varret, F.; Cartier dit Moulin, C.; Verdaguer, M. *J. Am. Chem. Soc.* **2000**, *122*, 6648. (c) Pejakovic, D. A.; Manson, J. L.; Miller, J. S.; Epstein, A. J. *Phys. Rev. Lett.* **2000**, *85*, 1994. (d) Goujon, A.; Roubeau, O.; Varret, F.; Dolbecq, A.; Bleuzen, A.; Verdaguer, M. *Eur. Phys. J. B* **2000**, *14*, 115.
(4) Arimoto, Y.; Ohkoshi, S.; Zhong, Z. J.; Seino, H.; Mizobe, Y.; Hashimoto, K. *J. Am. Chem. Soc.* **2003**, *125*, 9240.
(5) Ohkoshi, S.; Machida, N.; Zhong, Z. J.; Hashimoto, K. *Synth. Met.* **2001**, *122*, 523. (b) Ohkoshi, S.; Machida, N.; Abe, Y.; Zhong, Z. J.; Hashimoto, K. *Chem. Lett.* **2001**, 312.
(6) Rombaut, G.; Verelst, M.; Golhen, S.; Ouahab, L.; Mathonière, C.; Kahn, O. *Inorg. Chem.* **2001**, *40*, 1151. (b) Rombaut, G.; Mathonière, C.; Guionneau, P.; Golhen, S.; Ouahab, L.; Verelst, M.; Lecante, P. *Inorg. Chim. Acta* **2001**, *326*, 27. (c) Herrera, J. M.; Marvaud, V.; Verdaguer, M.; Marrot, J.; Kalisz, M.; Mathonière, C. *Angew. Chem., Int. Ed.* **2004**, *43*, 5468.
(7) Ohkoshi, S.; Einaga, Y.; Fujishima, A.; Hashimoto, K. *J. Electroanal. Chem.* **1999**, *473*, 245.
(8) Tokoro, H.; Ohkoshi, S.; Hashimoto, K. *Appl. Phys. Lett.* **2003**, *82*, 1245.
(9) Ohkoshi, S.; Yorozu, S.; Sato, O.; Iyoda, T.; Fujishima, A.; Hashimoto, K. *Appl. Phys. Lett.* **1997**, *70*, 1040.
(10) Verdaguer, M.; Bleuzen, A.; Marvaud, V.; Vaissermann, J.; Seuleiman, M.; Desplanches, C.; Scuiller, A.; Train, C.; Garde, R.; Gelly, G.; Lomenech, C.; Rosenman, I.; Veillet, P.; Cartier, C.; Villain, F. *Coord. Chem. Rev.* **1999**, *192*, 1023. (b) Hashimoto, K.; Ohkoshi, S. *Philos. Trans. R. Soc. London, Ser. A* **1999**, *357*, 2977. (c) Miller, J. S. *MRS Bull.* **2000**, *25*, 60. (d) Ohba, M.; Ohkawa, H. *Coord. Chem. Rev.* **2000**, *198*, 313. (e) Smith, J. A.; Galan-Mascaros, J. R.; Clérac, R.; Sun, J. S.; Xiang, O. Y.; Dunbar, K. R. *Polyhedron* **2002**, *20*, 1727.
(11) Ferlay, S.; Mallah, T.; Ouahs, R.; Veillet, P.; Verdaguer, M. *Nature* **1995**, *378*, 701. (b) Holmes, S. M.; Girolami, G. S. *J. Am. Chem. Soc.* **1999**, *121*, 5593. (c) Hatlevik, Ø.; Bushmann, W. E.; Zhang, J.; Manson, J. L.; Miller, J. S. *Adv. Mater.* **1999**, *11*, 914. (d) Ohkoshi, S.; Mizuno, M.; Hung, G. J.; Hashimoto, K. *J. Phys. Chem. B* **2000**, *104*, 9365.
(12) Ohkoshi, S.; Iyoda, T.; Fujishima, A.; Hashimoto, K. *Phys. Rev. B* **1997**, *56*, 11642.
(13) Ohkoshi, S.; Abe, Y.; Fujishima, A.; Hashimoto, K. *Phys. Rev. Lett.* **1999**, *82*, 1285.
(14) Ohkoshi, S.; Hozumi, T.; Hashimoto, K. *Phys. Rev. B* **2001**, *64*, 132404.
(15) Ohkoshi, S.; Arai, K.; Sato, Y.; Hashimoto, K. *Nat. Mater.* **2004**, *3*, 857.

10.1021/ja044107o CCC: $30.25

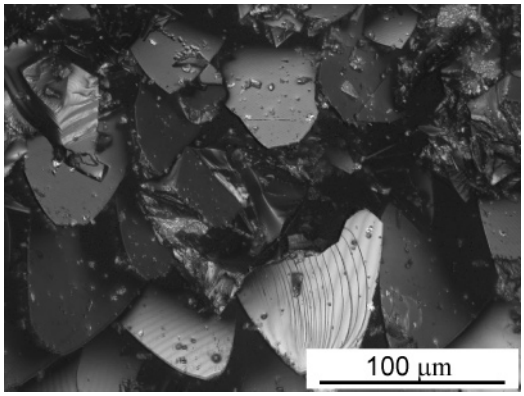

Figure 1. Photograph of electrochemically synthesized single crystals.

Table 1. Film Thickness and Total Charge Per Unit Area

total charge per unit area (mC/cm^2)	film thickness (μm)
10	0.2(1)
27	0.7(1)
50	1.3(1)
73	1.7(1)
96	2.4(1)
122	3.0(1)

different spatial configurations (e.g., square antiprism (D_{4h}), dodecahedron (D_{2d}), and bicapped trigonal prism (C_{2v})), depending on their chemical environment, such as the surrounding ligands.[16−30] In this work, we electrochemically synthesized a novel cyano-bridged copper−molybdenum complex, $Cs^{I}_2Cu^{II}_7[Mo^{IV}(CN)_8]_4{\cdot}6H_2O$, which exhibits photoinduced magnetization. Herein, we show the electrochemical synthesis, crystal structure, magnetic properties, and photofunctionality of this cyano-bridged $Cu^{II}-Mo^{IV}$ complex.

2. Experimental Section

2.1. Electrochemical Synthesis. The target material was electrochemically prepared by reducing a 30 cm^3 mixed aqueous solution of $Cu^{II}(NO_3)_2{\cdot}3H_2O$ (36 mg, 0.15 mmol) and $Cs_3[Mo^{V}(CN)_8]{\cdot}2H_2O$[31] (55 mg, 0.075 mmol) in a standard three-electrode cell at a constant potential condition of +500 mV vs Ag/AgCl electrode using a Hokuto-Denko HSV-100 potentiostat. The electrolytic aqueous solutions were adjusted to pH 3 with HNO_3. After 3 days, a single crystal of the compound was obtained on a Pt wire electrode (0.5 mm ϕ). A film-type of material was prepared on a SnO_2 (20 Ω/square)-coated glass with a loaded electrical capacity of 45−605 mC. Elemental analyses by an inductively coupled plasma mass spectroscopy (ICP-MS) and standard microanalytical methods confirmed that the formula of the single crystal was $Cs^{I}_2Cu^{II}_7[Mo^{IV}(CN)_8]_4{\cdot}6H_2O$. Calculated: Cs, 13.1; Cu, 21.9; Mo, 18.9; C, 18.9; N, 22.0%. Found: Cs, 12.3; Cu, 22.0; Mo, 18.4; C, 19.0; N, 21.5%. The formula of the film was consistent with that of the single crystal. Found: Cs, 12.4; Cu, 21.8; Mo, 18.4; C, 18.9; N, 21.3%.

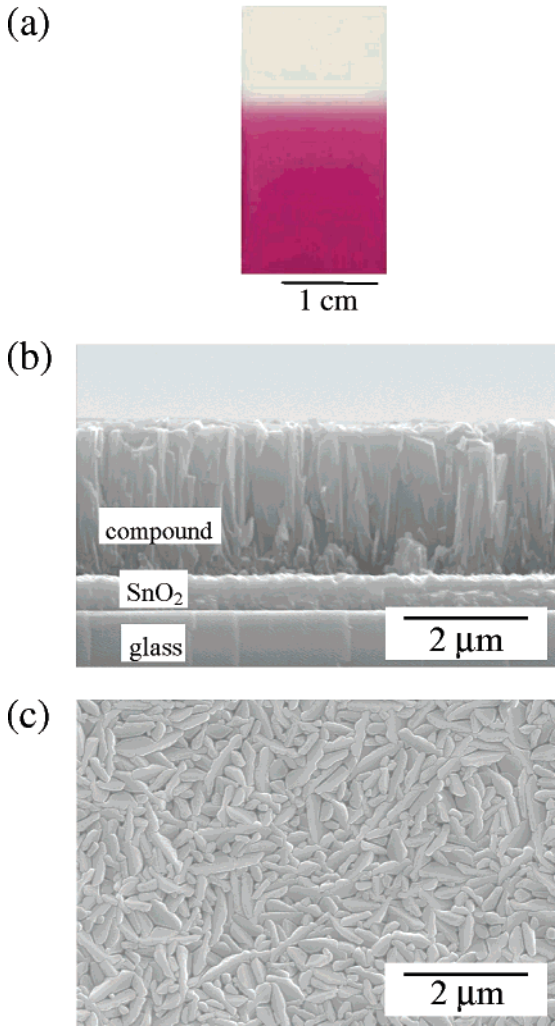

Figure 2. Electrochemically synthesized thin film: (a) photograph. (b) SEM image of the cross-section of the film. (c) SEM image of the top of view of the film.

2.2. Measurements. The film thickness was measured by a KEYENCE VF-7500 laser profile micrometer. The surface morphologies and cross sections of the thin films were measured by a Hitachi S-4200 scanning electron microscopy (SEM). The UV−visible absorption spectrum was measured by a Shimadzu UV-3100 spectrometer. The infrared spectra (IR) were recorded on a Shimadzu FT-IR 8200PC spectrometer. The X-ray powder diffraction (XRD) patterns were measured by a Rigaku RINT2100 spectrometer. The electron spin resonance (ESR) spectra were recorded at 103 K with a JEOL RE1X X-band ESR spectrometer. The determination of the unit cell and the collection of intensity data were made at 123 K on a Rigaku RAXIS−RAPID imaging plate with graphite monochromated Mo Kα radiation. Of the 8836 reflections that were collected, 701 were unique. The

(16) Zhong, Z. J.; Seino, H.; Mizobe, Y.; Hidai, M.; Fujishima, A.; Ohkoshi, S.; Hashimoto, K. *J. Am. Chem. Soc.* **2000**, *122*, 2952. (b) Larionova, J.; Gross, M.; Pilkington, M.; Andres, H.; Evans, H. S.; Güdel, H. U.; Decurtins, S. *Angew. Chem., Int. Ed.* **2000**, *39*, 1605. (c) Bonadio, F.; Gross, M.; Evans, H. S.; Decurtins, S. *Inorg. Chem.* **2002**, *41*, 5891.
(17) Rombaut, G.; Golhen, S.; Ouahab, L.; Mathonière, C.; Kahn, O. *J. Chem. Soc., Dalton Trans.* **2000**, 3609.
(18) Li, D. F.; Gao, S.; Zheng, L.; Tang, W. *J. Chem. Soc., Dalton Trans.* **2002**, 2805.
(19) Li, D. F.; Zheng, L.; Zhang, Y.; Huang, J.; Gao, S.; Tang, W. *Inorg. Chem.* **2003**, *42*, 6123.
(20) Podgajny, R.; Korzeniak, T.; Balanda, M.; Wasiutynski, T.; Errington, W.; Kemp, T. J.; Alcock, N. W.; Sieklucka, B. *Chem. Commun.* **2002**, 1138.
(21) Ohkoshi, S.; Arimoto, Y.; Hozumi, T.; Seino, H.; Mizobe, Y.; Hashimoto, K. *Chem. Commun.* **2003**, 2772.
(22) Hozumi, T.; Ohkoshi, S.; Arimoto, Y.; Seino, H.; Mizobe, Y.; Hashimoto, K. *J. Phys. Chem. B* **2003**, *107*, 11571.
(23) Li, D. F.; Zheng, L. M.; Wang, X. Y.; Huang, J.; Gao, S.; Tang, W. X. *Chem. Mater.* **2003**, *15*, 2094.
(24) Garde, R.; Desplanches, C.; Bleuzen, A.; Veillet, P.; Verdaguer, M. *Mol. Cryst. Liq. Cryst.* **1999**, *334*, 587.
(25) Zhong, Z. J.; Seino, H.; Mizobe, Y.; Hidai, M.; Verdaguer, M.; Ohkoshi, S.; Hashimoto, K. *Inorg. Chem.* **2000**, *39*, 5095.
(26) Li, D. F.; Gao, S.; Zheng, L. M.; Sun, W. Y.; Okamura, T.; Ueyama, N.; Tang, W. X. *New J. Chem.* **2002**, *26*, 485.
(27) Song, Y.; Ohkoshi, S.; Arimoto, Y.; Seino, H.; Mizobe, Y.; Hashimoto, K. *Inorg. Chem.* **2003**, *42*, 1848.
(28) Herrera, J. M.; Bleuzen, A.; Dromzée, Y.; Julve, M.; Lloret, F.; Verdaguer, M. *Inorg. Chem.* **2003**, *42*, 7052.
(29) Kashiwagi, T.; Ohkoshi, S.; Seino, H.; Mizobe, Y.; Hashimoto, K. *J. Am. Chem. Soc.* **2004**, *126*, 5024.
(30) Bennett, M. V.; Long, J. R. *J. Am. Chem. Soc.* **2003**, *125*, 2394.
(31) Bok, L. D. C.; Leipoldt, J. G.; Basson, S. S. *Z. Anorg. Allg. Chem.* **1975**, *415*, 81.

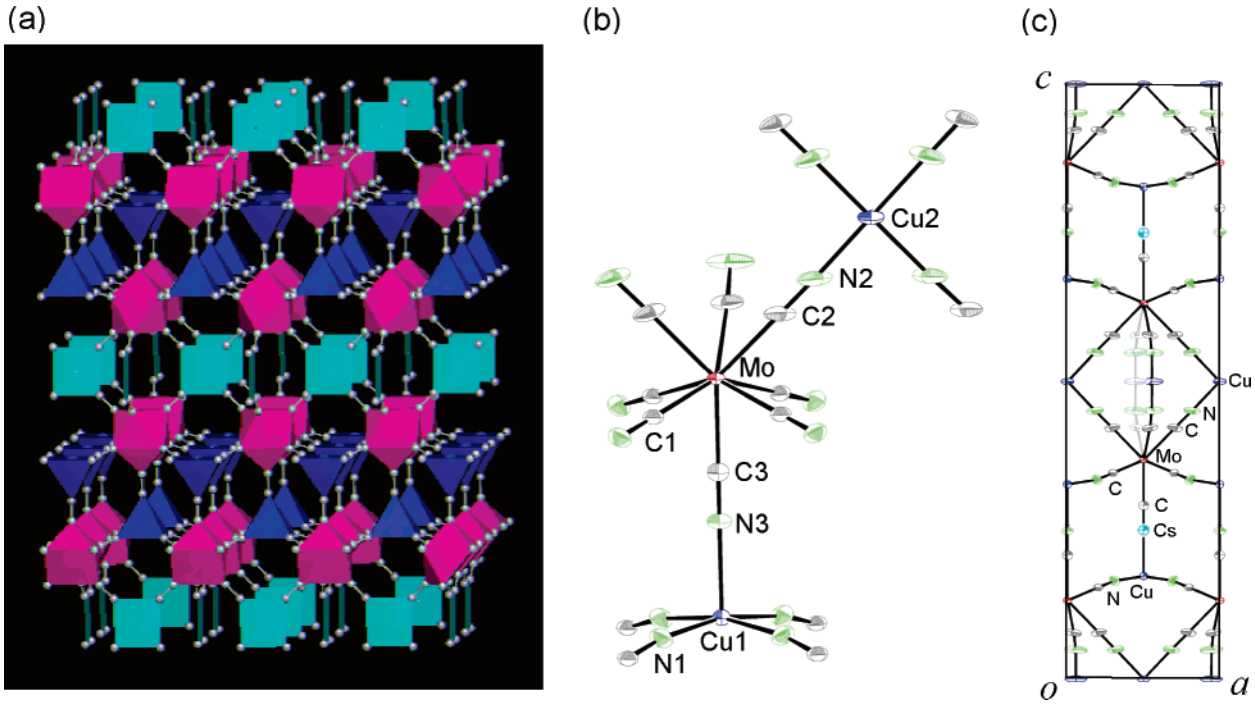

Figure 3. (a) Three-dimensional crystal structure using polyhedral model. Pink, blue, and light-blue polyhedron show MoC_8, $Cu1N_5$, and $Cu2N_4$, respectively. Water molecules and cesium atoms are omitted for clarity. (b) ORTEP drawing of the coordination environments around Cu and Mo. Blue, red, gray, and yellow−green ellipsoids represent Cu, Mo, C, and N, respectively. Displacement ellipsoids are drawn at a 50% probability level. Cu2, C2, and N2 atoms are disordered, and only selected atoms are drawn for clarity. (c) ORTEP drawing of the unit cell. Blue, red, light-blue, gray, and yellow−green ellipsoids represent Cu, Mo, Cs, C, and N, respectively. Displacement ellipsoids are drawn at a 50% probability level. Water molecules are omitted for clarity.

structure was solved by direct methods using SHELXS-97.[32] All non-hydrogen atoms were refined anisotropically. All calculations were performed using a teXsan crystallographic software package of Molecular Structure Corporation.[33] Magnetic susceptibility and magnetization measurements were conducted using a Quantum Design MPMS 7 superconducting quantum interference device (SQUID) magnetometer. The experimental conditions of the light irradiation measurements in SQUID, IR, ESR, and XRD spectrometries are as follows. In the SQUID measurement, a film-type of the compound was placed on the edge of an optical fiber, and a filtered blue light (450−500 nm, 5 mW/cm^2, 24 h) of a Xe lamp was used at 5 K. IR measurement was carried out using a film-type of the compound in the range of 1000−4000 cm^{-1} using a Xe lamp (450−500 nm, 10 mW/cm^2, 6.5 h) at 3 K. In the ESR measurement, a film-type of the compound was irradiated using a 473 nm light of a CW diode laser (115 mW/cm^2, 0.75 h) at 103 K. In the XRD measurement, a crashed sample of the film-type of the compound was irradiated using a Xe lamp (450−500 nm, 6 mW/cm^2, 24 h) at 15 K.

3. Results and Discussion

3.1. Materials. Dark purple single crystals that were 70 ± 30 μm were obtained on a Pt wire electrode (Figure 1). Purple thin films were obtained on SnO_2-coated glasses, as shown in Figure 2a. The thickness of the prepared films depended on the total charge per unit area, as shown in Table 1. Measurements by a laser profile micrometer showed that the roughness of the film surface was c.a. 0.1 μm in any obtained films, indicating that the surface of the films was smooth. SEM images also showed that the film surface was smooth and homogeneous over the entire area of the film (1.5 × 2.0 cm^2) (Figure 2b,c).

The electrochemical growth of this compound is caused by the reduction of the $[Mo^V(CN)_8]^{3-}$ ion. Since the redox potential of $[Mo^{IV/V}(CN)_8]^{4-/3-}$ is +580 mV vs Ag/AgCl electrode,[34] $[Mo^V(CN)_8]^{3-}$ is reduced to $[Mo^{IV}(CN)_8]^{4-}$ on the surface of the working electrode at a constant potential of +500 mV. Then, the produced $[Mo^{IV}(CN)_8]^{4-}$ reacts with Cu^{2+} ions, which results in the crystal of the cyano-bridged $Cu^{II}-Mo^{IV}$ complex being deposited on the electrode, as described by the following electrochemical reactions.

$$[Mo^V(CN)_8]^{3-} + e^- \rightarrow [Mo^{IV}(CN)_8]^{4-} \quad (1)$$

$$4[Mo^{IV}(CN)_8]^{4-} + 7Cu^{2+} + 2Cs^+ \rightarrow Cs^I_2Cu^{II}_7[Mo^{IV}(CN)_8]_4\cdot 6H_2O \quad (2)$$

3.2. Crystal Structure. X-ray single-crystal structural analysis shows that this compound consists of a three-dimensional cyano-bridged Cu−Mo bimetallic assembly with a tetragonal structure of *I*4/*mmm* space group ($a = b = 7.2444(9)$ Å, $c = 28.417(5)$ Å, and $Z = 1$) (Figure 3a). Table 2 lists the crystallographic data. Figure 3b,c shows the coordination environments around Mo and Cu and a unit cell of the crystal structure, respectively. This crystal has one coordination geometry for the Mo atom and two coordination geometries for the Cu atoms (Cu1 and Cu2). A Mo ion links five Cu1 ions and three Cu2 ions through CN ligands. The coordination geometry of MoC_8 adopts a bicapped trigonal prism geometry, and the Mo−C bond distances range from 2.148(4) to 2.171(9) Å. The Cu1 ion is coordinated to five cyanonitrogens, and its geometry is square pyramidal, in which the distances of the equatorial Cu1−N1 and the apical Cu1−N3 are 1.977(4) and 2.233(7) Å, respectively. The Cu2 ion is coordinated to four cyanonitrogens, and it has a square planar geometry with a Cu2−N2 bond distance of 1.923(8) Å. As shown in Figure 4a,

(32) Sheldrick, G. M. *SHELXS 97, Program for Crystal Structure Determination. Acta Crystallogr.* **1990**, *A46*, 467.
(33) *teXsan: Crystal Structure Analysis Package*; Molecular Structure Corporation, 1985, 1992.
(34) Samotus, A.; Szklarzewicz, J. *Coord. Chem. Rev.* **1993**, *125*, 63.

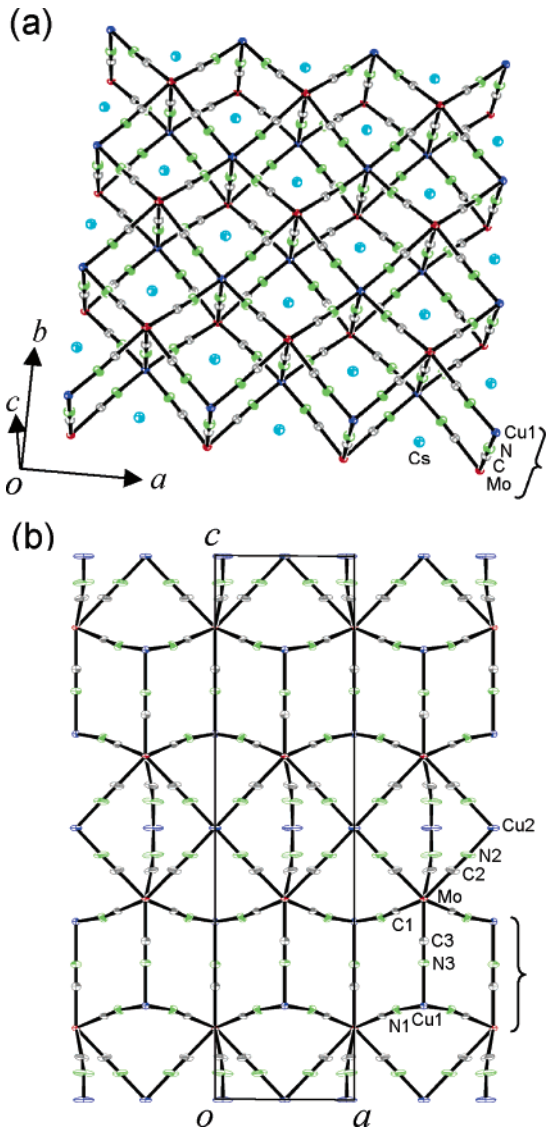

Figure 4. Crystal structure of $Cs_2Cu_7[Mo(CN)_8]_4 \cdot 6H_2O$. Blue, red, light-blue, gray, and yellow−green ellipsoids represent Cu, Mo, Cs, C, and N, respectively. Displacement ellipsoids are drawn at a 50% probability level. (a) Structure of cyano-bridged $\{Cu[Mo(CN)_5]\}_n$ double-layer. The occupancy of cesium atom is 50%. (b) Projection of three-dimensional network viewed toward the *b* axis. Water molecules and cesium atoms are omitted for clarity.

Table 2. Crystallographic Data

chemical formula	$C_{32}H_{12}N_{32}O_6Cs_2Cu_7Mo_4$
formula weight	2035.04
crystal system	tetragonal
space group	*I*4/*mmm* (No. 139)
a/Å	7.244(9)
b/Å	7.244(9)
c/Å	28.417(5)
V/Å^3	1491.4(4)
Z	1
D_{calcd}/g cm^{-3}	2.266
T/K	123
λ/Å	0.71069
μ/cm^{-1}	45.20
R^a	0.0305
wR^a	0.0750

[a] $R = \sum||F_o| - |F_c||/\sum|F_o|$; $wR = [\sum(w(F_o^2 - F_c^2)^2)/\sum w(F_o^2)^2]^{1/2}$.

Cu1 and Mo form the square-grid layer through the cyanides in the *ab* plane, and the axial cyanide of $Cu1(NC)_5$ connects the upper (or lower) grid layer, which forms a double-layer

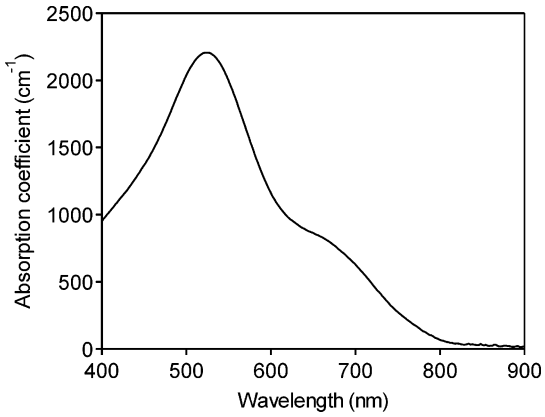

Figure 5. UV−visible absorption spectrum of an electrochemically synthesized film.

structure. The cesium ion occupies the cubic cavity of this double layer with an occupancy of $^1/_2$. Three out of the eight cyanides that surround the Mo ions stand out of the double-layer and connect to Cu2 ions (Figure 4b). There are eight symmetry equivalent positions of Cu2 on the plane of $z = {}^1/_2$. Thus, the occupancies of C2, N2, and Cu2 atoms are $^3/_8$ (see Supporting Information). The distances between the Cu and Mo ions are 5.252 (Mo−C1−N1−Cu1), 5.549 (Mo−C3−N3−Cu1), and 5.228 Å (Mo−C2−N2−Cu2). Water molecules are between the double-layers as zeolitic water molecules.

3.3. Spectroscopic and Magnetic Properties. The CN stretching frequency was observed at 2163 cm^{-1} in the IR spectra for both the film-type and the crystal-type of the compound at room temperature. On the basis of the IR data of bridging cyanide previously reported (ν_{CN} = 2162−2124 cm^{-1}),[5,6,35,36] this peak is assigned to the CN stretching peak of $Mo^{IV}-CN-Cu^{II}$. Figure 5 shows a UV−visible absorption spectrum of the film prepared at a total charge per unit area of 96 mC/cm^2 (d = 2.4(1) μm). This compound possesses absorption bands near 520 nm with an absorption coefficient (α) of 2200 cm^{-1} and 650 nm with α = 850 cm^{-1}. The absorption at 650 nm is assigned to a d−d transition of Cu^{II} ($^2B_1 \rightarrow {}^2B_2$ in square pyramidal Cu1 and/or $^2B_{1g} \rightarrow {}^2A_{1g}$ in square planar Cu2). In light of the previous papers,[5a,6a,37] the other absorption at 520 nm is assigned to an intervalence transfer (IT) band between $Mo^{IV}-CN-Cu^{II}$ and $Mo^{V}-CN-Cu^{I}$.

The ESR spectra of the film at room temperature show one dispersive peak with a g value of 2.14 and line width of 180 G, which is probably due to paramagnetic Cu^{II} ($S = {}^1/_2$). Figure 6a shows the temperature dependence of the molar magnetic susceptibility (χ_M) under an applied field of 5000 G. The $\chi_M T$ value at 300 K is equal to 3.1 cm^3 mol^{-1} K, which almost corresponds to the expected spin-only moment value of 3.0 cm^3 mol^{-1} K for $S = {}^1/_2$ and g_{Cu} = 2.14. As the temperature decreases, the $\chi_M T$ value is almost constant until 10 K, and then it decreases. The observed χ_M values obey the Curie−Weiss law (i.e., $\chi_M = C/(T - \theta)$) in the range of 10−300 K with a Weiss constant (θ) of −0.42 K and a Curie constant (C) of 3.13 cm^3 mol^{-1} K (Figure 6b). The negative sign of the θ value

(35) Li, D. F.; Yang, D. X.; Li, S. H.; Tang, W. X. *Inorg. Chem. Commun.* **2002**, *5*, 791.
(36) Podgajny, R.; Korzeniak, T.; Stadnicka, K.; Dromzée, Y.; Alcock, N. W.; Errington, W.; Kruczała, K.; Bałanda, M.; Kemp, T. J.; Verdaguer, M.; Sieklucka, B. *J. Chem. Soc., Dalton Trans.* **2003**, 3458.
(37) Hennig, H.; Rehorek, A.; Rehorek, D.; Thomas, P. *Inorg. Chim. Acta* **1984**, *86*, 41.

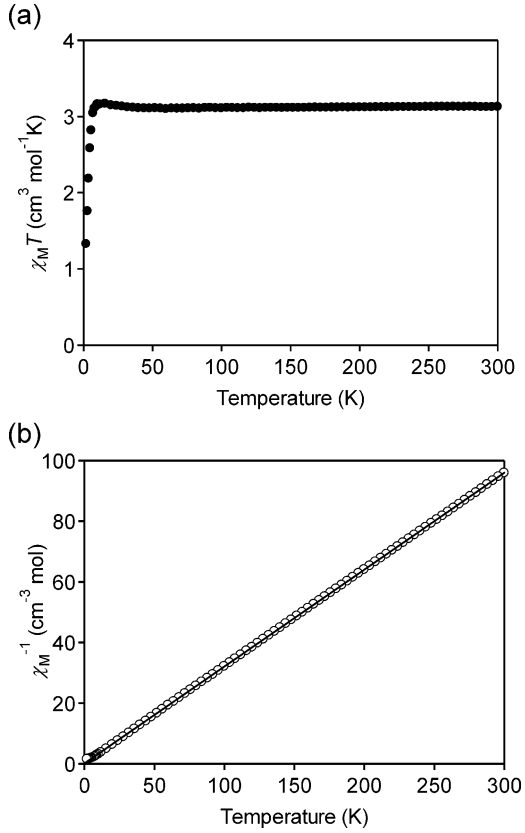

Figure 6. Temperature dependence of the magnetic susceptibility measured under an external magnetic field of 5000 G. (a) $\chi_M T$ vs temperature plots. (b) $\chi_M{}^{-1}$ vs temperature plots. The solid line represents the fitting line using Curie−Weiss law.

suggests that the magnetic interaction between the Cu^{II} through the diamagnetic $-NC-Mo^{IV}(S = 0)-CN-$ bridge is weak antiferromagnetic coupling.

3.4. Photomagnetic Properties. When the sample was irradiated with blue light (450−500 nm) at 5 K, a spontaneous magnetization with a Curie temperature (T_C) of 23 K and a magnetic hysteresis loop with coercive field (H_c) of 350 G were observed (Figure 7). The temperature dependences of the remanent magnetization (RM) curve and the field-cooled magnetization (FCM) curve were almost the same, as shown in Figure 7a. This indicates that the magnetization increase below 23 K is due to the ferromagnetic ordering. Warming the sample to 200 K returned the magnetic properties to the initial state. This photomagnetic behavior was repeatedly observed, indicating that the magnetization can be induced by a photon mode and recovered by a thermal mode.

To understand the mechanism of this photomagnetic behavior, IR and ESR spectra after irradiating were measured. Figure 8 shows IR spectra when irradiating with blue light (450−500 nm) at 3 K. Irradiating decreased the IR peak due to $Mo^{IV}-CN-Cu^{II}$ at 2171 cm^{-1},[38] and when the sample was warmed above 300 K and cooled to 3 K, the IR spectra were identical to the spectra before irradiating. Irradiating with 473 nm light at 103 K decreased the ESR peak due to Cu^{II}, as shown in Figure 9. The signal intensity returned to the initial value after a thermal treatment of 300 K. These results indicate that irradiating decreases the number of Mo^{IV} and Cu^{II}.

(38) With decreasing temperature, the CN stretching peak gradually shifted from 2163 cm^{-1} at room temperature to 2171 cm^{-1} at 3 K due to the volume contraction.

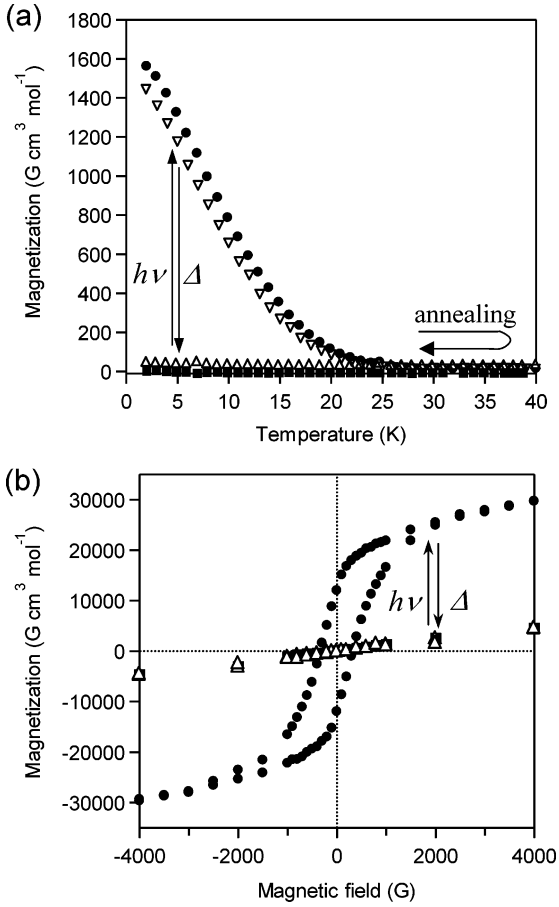

Figure 7. (a) Magnetization vs temperature curves in the magnetic field of 10 G before light irradiation (■), after light irradiation (●), and after thermal treatment of 200 K (△). Remanent magnetization (▽) of the irradiated sample was measured with increasing temperature after the temperature decreased at 10 G. (b) Magnetic hysteresis loop at 2 K before (■) and after light irradiation (●), and after thermal treatment at 200 K (△).

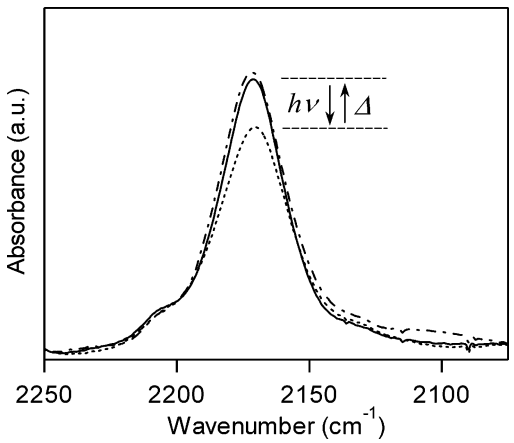

Figure 8. IR spectra at 3 K before light irradiation (—), after light irradiation (• • •), and after thermal treatment of 300 K (-•-•-).

The photoinduced magnetization of this compound can be explained by the following mechanism. The compound in the initial state is paramagnetic. Irradiating excites the compound to a charge transfer state. The compound in the excited state immediately relaxes to the initial state or forms the valence isomer ($Mo^V-CN-Cu^I$) state. In the present system, the decrease of the number of Mo^{IV} and Cu^{II} indicates the change from $Mo^{IV}-CN-Cu^{II}$ to $Mo^V-CN-Cu^I$. In this valence isomer

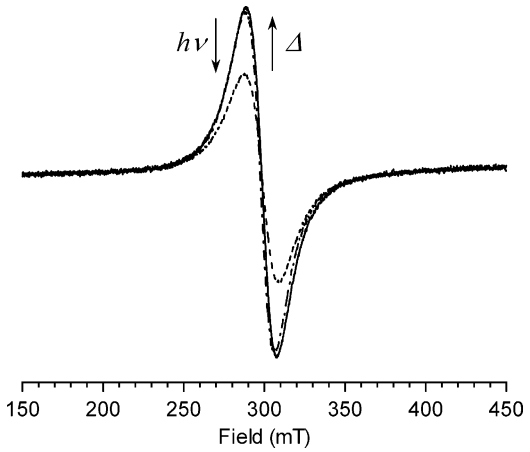

Figure 9. ESR spectra at 103 K before light irradiation of 473 nm (—), after light irradiation (· · ·), and after thermal treatment of 300 K (-·-·-).

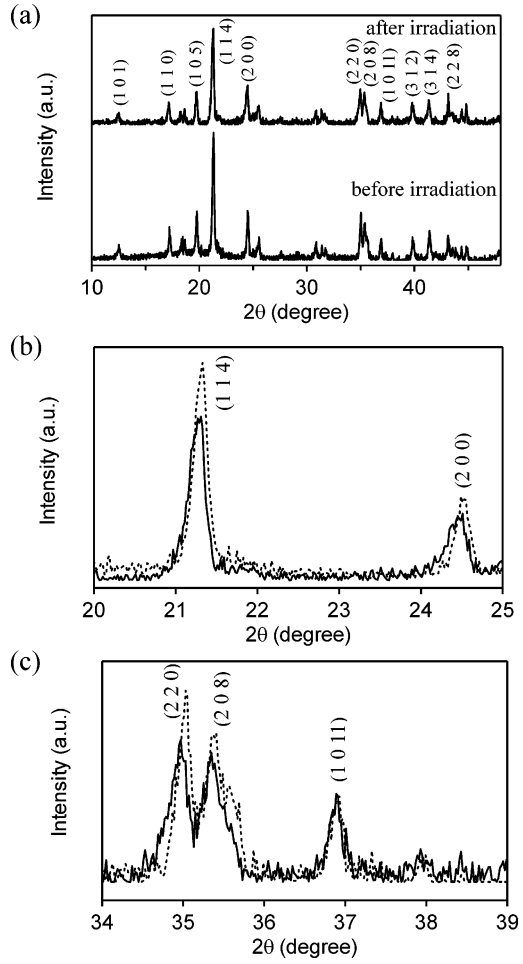

Figure 10. (a) XRD spectra before (bottom) and after (top) the light irradiation at 15 K. Panels b and c are enlarged plots of a. Before (- - -) and after irradiation (—).

state, the Mo^{V} ($4d^1$, $S = {}^1/_2$) has an unpaired electron, but Cu^{I} ($3d^{10}$, $S = 0$) does not have an unpaired electron. However, ${}^3/_7$ of the copper ions should remain as Cu^{II} due to the stoichiometric limitation in the present compound, that is, the irradiated compound is expressed as $Cs^{I}_2Cu^{I}_4Cu^{II}_3[Mo^{V}(CN)_8]_4{\cdot}6H_2O$. Consequently, the produced Mo^{V} is coordinated to an average of 3.42 ($8 \times {}^3/_7$) of Cu^{II} after the electron transfer is accomplished. A spontaneous magnetization appears to be due to the ferromagnetic coupling between the unpaired electrons

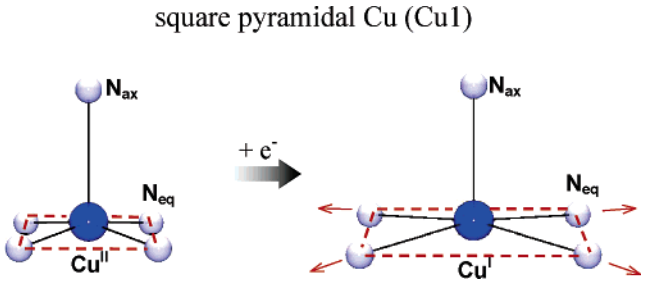

Figure 11. Schematic illustration of the change in bond distances for five-coordinated square pyramidal Cu1 by the reduction from Cu^{II} to Cu^{I}.

on the Mo^{V} ($S = {}^1/_2$) and those on the Cu^{II} ($S = {}^1/_2$) of the irradiated compound.

To investigate the structural changes, the XRD pattern with the light irradiation was also measured. Irradiating with blue light (450−500 nm) at 15 K caused some XRD peaks (e.g., (1 1 4), (2 0 0), (2 2 0), and (2 0 8)) to shift to a lower angle, but some XRD peaks (e.g., (1 0 11)) did not shift, as shown in Figure 10. The lattice constant of a ($= b$) axis increased from 7.242(3) to 7.255(5) Å, while that of c axis (28.44 Å) remained the same. When the irradiated sample was warmed above 300 K and then cooled to 15 K, the XRD pattern returned to the initial pattern. This anisotropic structure expansion when irradiating suggests that the electron transfer from Mo^{IV} to square pyramidal Cu^{II} (Cu1) is dominant in this photoreaction since (i) square planar Cu^{I} is unstable and cannot exist even if square planar Cu^{II} (Cu2) accepts an electron from Mo^{IV}, and (ii) the equatorial bond distance in square pyramidal Cu^{II} should be elongated when Cu^{II} is reduced to Cu^{I} (Figure 11).[39] When the present photomagnetic phase is compared to that of $Cu_2[Mo(CN)_8]{\cdot}8H_2O$ ($T_C = 30$ K, $H_c = 7$ G)[5a], the H_c value is remarkably improved (i.e., $H_c = 350$ G). This may be related to the double-layer structure formed by an introducing a Cs ion to cyano-bridged Cu−Mo system.

4. Conclusion

Single crystal- and film-types of a three-dimensional cyano-bridged Cu−Mo bimetallic assembly, $Cs^{I}_2Cu^{II}_7[Mo^{IV}(CN)_8]_4{\cdot}6H_2O$, were electrochemically prepared. When the compound was irradiated with 450−500 nm light at 5 K, a spontaneous magnetization with a Curie temperature of 23 K was observed. In this photoinduced magnetization, ferromagnetic ordering between Mo^{V} ($S = {}^1/_2$) and Cu^{II} ($S = {}^1/_2$) was produced by exciting the intervalence transfer band between molybdenum and copper.

Acknowledgment. The present research is supported in part by a grant for 21st Century COE Program, *Human-Friendly Materials based on Chemistry*, and a Grand-in-Aid for Scientific Research from the Ministry of Education, Culture, Sports, Science, and Technology of Japan.

Supporting Information Available: X-ray crystallographic file in CIF format. Information relating to the disordered crystal structure, Faraday spectra, and temperature dependence of the lattice constant. This material is available free of charge via the Internet at http://pubs.acs.org.

JA044107O

(39) Holloway, C. E.; Melnik, M. *Rev. Inorg. Chem.* **1995**, *15*, 147.